JB
Journals.ASM.org

Analysis of the CtrA Pathway in *Magnetospirillum* Reveals an Ancestral Role in Motility in Alphaproteobacteria

Shannon E. Greene,[a] Matteo Brilli,[b] Emanuele G. Biondi,[c] and Arash Komeili[a]

Plant and Microbial Biology, University of California, Berkeley, Berkeley, California, USA[a]; INRIA Rhone-Alpes and Laboratoire de Biométrie et Biologie Evolutive, UMR CNRS 5558, Université Lyon 1, Villeurbanne, France[b]; and Interdisciplinary Research Institute, CNRS-Univ. Lille1-Lille2, Villeneuve d'Ascq, France[c]

Developmental events across the prokaryotic life cycle are highly regulated at the transcriptional and posttranslational levels. Key elements of a few regulatory networks are conserved among phylogenetic groups of bacteria, although the features controlled by these conserved systems are as diverse as the organisms encoding them. In this work, we probed the role of the CtrA regulatory network, conserved throughout the *Alphaproteobacteria*, in the magnetotactic bacterium *Magnetospirillum magneticum* strain AMB-1, which possesses unique intracellular organization and compartmentalization. While we have shown that CtrA in AMB-1 is not essential for viability, it is required for motility, and its putative phosphorylation state dictates the ability of CtrA to activate the flagellar biosynthesis gene cascade. Gene expression analysis of strains expressing active and inactive CtrA alleles points to the composition of the extended CtrA regulon, including both direct and indirect targets. These results, combined with a bioinformatic study of the AMB-1 genome, enabled the prediction of an AMB-1-specific CtrA binding site. Further, phylogenetic studies comparing CtrA sequences from alphaproteobacteria in which the role of CtrA has been experimentally examined reveal an ancestral role of CtrA in the regulation of motility and suggest that its essential functions in other alphaproteobacteria were acquired subsequently.

The past decades have proved exciting for bacterial cell biology, since the mechanisms underlying subcellular organization and developmental processes in microorganisms have been increasingly uncovered. Developmental processes include flagella, pili, and secretion system biogenesis, while subcellular organization is exemplified by cytoskeletal elements which coordinate chromosome replication, cell wall synthesis, and even the organization of intracellular organelles (17, 35, 54). The temporal and spatial regulation of developmental events across the bacterial cell cycle has been investigated most thoroughly in the alphaproteobacterium *Caulobacter crescentus*. The proper execution of *C. crescentus* asymmetric cell division requires timed coordination of gene expression, protein activation, and assembly of polar organelles, as well as physical partitioning in different parts of the cell proteins which regulate these processes (18). Coordination of these events involves a regulatory network of proteins that activate or repress one another through gene expression, posttranslational modification, and protein stability (9). At the core of this network is the response regulator and transcription factor CtrA.

In *C. crescentus*, *ctrA* is an essential gene, whose product is tightly regulated at the levels of gene expression, protein activation, and proteolysis (9). CtrA represses initiation of DNA replication by directly binding several sites flanking the origin of replication (39). Additionally, CtrA acts as a transcription factor to directly control the expression of a quarter of cell cycle-regulated genes in *C. crescentus*, including genes involved in DNA methylation, cell division, signal transduction, and motility (29, 30, 50). CtrA activity depends on the phosphorylation state of a conserved aspartate residue; phosphorylation of CtrA through the histidine kinase response regulator CckA and the histidine phosphotransferase ChpT enables CtrA to bind and inhibit the origin of replication, as well as activating or repressing gene promoters, including its own, at specific recognition sites (3, 11, 47). Phosphate flow to CtrA via CckA is inhibited by the essential response regulator DivK, whose transcription is also under CtrA control (3, 7).

In addition to its essential role in the progression of the *C. crescentus* cell cycle, CtrA homologs in *Sinorhizobium meliloti*, *Agrobacterium tumefaciens*, and *Brucella abortus* have been shown or suggested to be essential for viability (1, 2, 23, 40). In contrast, in *Rhodobacter capsulatus*, *Rhodospirillum centenum*, and *Silicibacter* sp. TM1040, *ctrA* can be disrupted with no adverse effects on the division cycle or cell survival but is essential for regulating motility (4, 27, 33, 34, 46). The disparate roles of CtrA in various members of the *Alphaproteobacteria* raises questions about the flexibility of regulatory networks, in which certain components are conserved and yet play vastly different roles in the cell (6). What role might the response regulator CtrA play in an organism, for example, which possesses subcellular compartmentalization? If CtrA functions to direct polar organelle biogenesis and cell division in some alphaproteobacteria, perhaps it may direct the fates of bacterial organelles in others. Here we have explored the regulatory network controlled by CtrA in the magnetotactic alphaproteobacterium *Magnetospirillum magneticum* sp. AMB-1 (AMB-1), an organism capable of forming intracellular organelles.

Magnetotactic bacteria (MB) are a diverse group of prokaryotes which biomineralize chains of magnetosomes, membrane-enclosed magnetic crystals, within their cells, allowing these bacteria to align with the geomagnetic field and locate microaerobic environments more efficiently in a process termed magne-

Received 6 February 2012 **Accepted** 22 March 2012
Published ahead of print 30 March 2012
Address correspondence to Arash Komeili, komeili@berkeley.edu.
Supplemental material for this article may be found at http://jb.asm.org/.

doi:10.1128/JB.00170-12

TABLE 1 Strains of AMB-1 used in this work

Strain no.	Description	Source or reference
AK30	AMB-1 wild type	32
AK31	ΔMAI; spontaneous magnetosome island deletion	36
AK115	Δ*ctrA*	This work
AK116	Δ*divK*	This work
AK117	Δ*ctrA* ΔMAI	This work

TABLE 2 Plasmids generated in this work

Plasmid name	Origin	Expt	Antibiotic(s)
pAK607	pAK0 derived	Deletion of *ctrA* (*amb0629*)	Kan
pAK614	pAK0 derived	Deletion of *divK* (*amb3570*)	Kan
pAK611	pAK22 derived	Complementation of Δ*ctrA*, WT allele	Kan, Amp
pAK612	pAK22 derived	Complementation of Δ*ctrA*, D51A allele	Kan, Amp
pAK613	pAK22 derived	Complementation of Δ*ctrA*, D51E allele	Kan, Amp
pAK617	pAK22 derived	Complementation of Δ*ctrA*, empty	Kan, Amp

toaerotaxis. Biochemical and genetic analyses of magnetotactic species, such as *Magnetospirillum magneticum* AMB-1, have identified a number of proteins that participate in magnetic mineral biomineralization, magnetosome "activation," and magnetosome alignment (25, 26, 36, 45). Genes encoding most of the known magnetosome proteins are found in a genomic region conserved across magnetotactic bacteria; this 98-kb genomic region is essential for magnetosome formation in AMB-1 and is termed the magnetosome island (MAI) (15, 36, 52). While progress has been made in uncovering genes specific to steps of magnetosome formation, the integration of these processes within the global regulatory circuits of the organism is poorly understood. In this study, we took a targeted approach to investigate the global regulation of CtrA in the context of a microorganism possessing intracellular organelles by generating deletions of homologs of known cell cycle control genes: *ctrA* and *divK*. Interestingly, while *ctrA* and *divK* are not essential for viability or cell cycle progression in AMB-1, the deletion strains have motility defects indicating conservation of the CtrA phosphorylation pathway in flagellar biosynthesis. A *ctrA* deletion in a hypermotile magnetosome island deletion strain abolishes motility, while a deletion of CtrA's negative regulator *divK* induces motility in a previously nonmotile wild-type (WT) genetic background. Global gene expression analysis of *ctrA* and *divK* deletion strains, as well as *ctrA* deletions complemented with active and inactive *ctrA* alleles, has revealed a novel CtrA regulon in AMB-1.

MATERIALS AND METHODS

Growth conditions. *Magnetospirillum magneticum* strain AMB-1 was grown in magnetospirillum growth medium (MG) under microaerobic conditions, as previously described (36). AMB-1 was grown in conical tubes filled with MG medium and incubated at 30°C. On plates, AMB-1 was grown on MG containing 0.7% agar, and medium was supplemented with antibiotics as follows: kanamycin on solid medium at 15 μg/ml, kanamycin in liquid medium at 7 μg/ml, and carbenicillin in liquid medium at 20 μg/ml. For growth curves, AMB-1 was grown in 10 ml MG medium in 20-ml culture tubes and incubated at 30°C in a microaerobic chamber in which the oxygen concentration was kept below 10%. After 2 days of growth, cultures were diluted to an optical density at 400 nm (OD_{400}) of 0.02 in fresh MG medium and returned to the microaerobic growth chamber. OD_{400} and coefficient of magnetism (Cmag) measurements (performed as described previously) were assayed every 90 min (26). Briefly, optical densities of cultures are assessed with a bar magnet placed parallel or perpendicular to the light path in the spectrophotometer. Cmag values are expressed as a ratio of parallel to perpendicular OD_{400} values; thus, a Cmag of 1 indicates a nonmagnetic culture.

Strain construction and complementation. Strains are listed in Table 1. All cloning was performed with *Escherichia coli* DH5α λpir grown in LB medium. The antibiotic kanamycin was used at 50 μg/ml. Gene deletions in *M. magneticum* AMB-1 were obtained via a two-step recombination method as described previously (36). A region (approximately 1,000 bp) upstream of each target gene was PCR amplified with BglII and BamHI restriction sites at the 5′ and 3′ ends, respectively. Similarly, a region (approximately 1,000 bp) downstream of the target gene was PCR amplified with BamHI and SpeI restriction sites at the 5′ and 3′ ends, respectively. These fragments were cloned in two steps into the BamHI and SpeI restriction sites of pAK0, a suicide plasmid carrying a kanamycin resistance cassette and the *sacB* gene, to yield vectors for deleting *ctrA* (*amb0629*) and *divK* (*amb3750*), respectively (Table 2). The plasmids were transferred to AMB-1 using conjugation via *E. coli* WM3064, and the transconjugants were selected for on MG plates containing kanamycin. Transconjugants were grown in liquid MG medium, and deletion mutants were selected for on MG plates containing 2% sucrose. The sucrose-resistant colonies were screened for the desired deletion and the absence of the kanamycin resistance cassette and *sacB* gene by PCR (36).

ctrA deletion strains were complemented by expressing WT, CtrA D51E, or D51A alleles from the *tac* promoter. Wild-type *ctrA* was PCR amplified and cloned into the expression vector pAK22 (25) using the EcoRI and SpeI restriction sites downstream of the *tac* promoter. The D51E and D51A alleles were generated following the Stratagene QuikChange PCR protocol. The gene conferring ampicillin resistance (*bla*), expressed downstream of a second *tac* promoter, was subsequently cloned using the SpeI restriction site, since increased complementation had been found to result when selecting on carbenicillin rather than kanamycin in AMB-1 (36). An empty-vector negative control was constructed by mutating the EcoRI restriction site upstream of *ctrA* in the complementation vector to a SpeI site; *ctrA* was then excised by SpeI digestion followed by self-ligation.

All primers are listed in Table S1 in the supplemental material.

Synchronization of AMB-1. Exponentially growing cells were passaged in 4 50-ml conical tubes until mid-exponential phase (OD_{400}, 0.07 to 0.09). Continuous Percoll gradients were established in 15-ml conical tubes by centrifuging 10 ml 50% Percoll-MG solution (100% Percoll represents 90% Percoll diluted by 10% 10× MG salts) at 10,000 × *g* for 30 min. AMB-1 cells were harvested by pelleting at 8,000 × *g* for 10 min, pooling the pellets in a single 1.5-ml Eppendorf tube. Cells were further concentrated by centrifugation at 16,000 × *g* for 2 min. Cells were resuspended in a 100-μl volume and loaded on the top of the gradient. Gradients were centrifuged in a swing rotor at 800 × *g* for 20 min. The top 500 μl, containing few cells, was removed, and the next 200-μl fraction was used to inoculate a 10-ml MG culture, which was grown in the microaerobic chamber. To verify synchronization of the culture, 100 μl was removed every 40 min for triplicate cell counts using a hematocytometer.

RNA extraction and cDNA synthesis. Exponentially growing cells were passaged in 50-ml conical tubes until exponential phase (OD_{400}, 0.04 to 0.08). Cells were vacuum filtered using a side-arm flask apparatus onto sterile Whatman Nuclepore Track-Etch membrane filters. Filters were removed with sterilized forceps and deposited in sterile microcentrifuge tubes, which were immediately plunge frozen in liquid nitrogen and stored thereafter at −80°C. RNA was extracted directly off the filters by

applying 1 ml TRIzol reagent to each microcentrifuge tube. Samples were mixed by vortexing and left to incubate for 5 min. Supernatants were then transferred to 2 ml Heavy Phase Lock tubes, to which 200 μl chloroform was added and mixed. Phase Lock tubes were spun at 4°C at 12,000 × *g* for 15 min, after which the supernatants were decanted into fresh microcentrifuge tubes. Five hundred microliters isopropanol was added, and the tubes were tilted gently for 10 min at room temperature before a second spin at 4°C of 12,000 × *g* for 15 min. The supernatant was removed, and the pellet was washed with 1 ml cold 75% ethanol and vortexed. Tubes were spun at 4°C at 7,500 × *g* for 5 min, and the supernatants were again removed. Pellets were air-dried for 10 min and then resuspended in 100 μl RNase-free water.

RNA quantity and quality were assessed using a NanoDrop spectrophotometer (Thermo Scientific). Samples were treated with DNase I (Invitrogen) and purified using the Qiagen RNeasy kit. Removal of genomic DNA was verified via PCR against two target genes. One microgram RNA was reverse transcribed using the Invitrogen SuperScript RT III kit as directed. Resulting cDNA was treated with RNase A (NEB) and RNase H (Invitrogen) to remove residual RNA and was purified using the Qiagen PCR cleanup kit and eluted in 10% elution buffer (EB). cDNA quantity and quality were assessed using a NanoDrop instrument.

Microarray sample preparation and array design. cDNA (0.5 μg) was fluorescently labeled with Cy3 using the Nimblegen One Color DNA labeling kit as directed. Labeling reaction mixtures were incubated at 37°C overnight in the dark. Labeling reactions were stopped as directed, and samples were resuspended in 25 μl nuclease-free water. Two micrograms Cy3-labeled cDNA was dried in a SpeedVac instrument at 30°C in the dark. Microarray sample hybridization and scanning were conducted at the Fred Hutchinson Cancer Research Center, Seattle, WA.

Our microarray consists of full coverage of the AMB-1 genome (GenBank accession no. NC_007626), with each gene covered by 7 60-nucleotide (nt) probes. The entire genomic probe set was duplicated on the array and in addition contained probe sets designed for 22 unannotated open reading frames (ORFs) in the magnetosome island (genomic coordinates 977403 to 1097027), with 7 60-nt probes per potential ORF. Potential ORFs in this genomic region were identified using the NCBI ORF Finder and are listed in Table 3. The microarray design also included tiling of the magnetosome island, from genomic coordinates 977403 to 1097027. This region was covered by 8,038 probes, 50 nt in length. However, results from these probes were not evaluated in this work.

Microarray data analysis. Scanned microarray images were processed using the ArrayScan software program (Nimblegen). .pair files were generated for all arrays in the data set, which were then normalized together using quantile normalization as described previously (5); gene calls were generated using the robust multichip average (RMA) algorithm (20, 21). Gene expression changes between strains were considered significant if an average change across three biological replicates was greater than 1.5-fold above or below the average for three biological replicates of the comparison strain. Select targets of interest were chosen from among the list of significantly upregulated genes for confirmation with quantitative reverse transcription-PCR (RT-PCR).

TaqMan RT-PCR. Primer and probe sets for each target gene and endogenous gyrase control were designed using the Primer Express software program (Applied Biosystems). Primer pair concentrations (900 nM, 300 nM, and 100 nM) were tested with a standard probe concentration (250 nM) for optimal dilution curves against genomic DNA. Optimized primer/target–6-carboxy-fluorescein (FAM) probe sets were tested in multiplex reactions against the gyrase-VIC internal controls in 50-μl reaction mixtures. Multiplex TaqMan reaction mixtures contained 2× Gene Expression master mix (Applied Biosystems), 250 nM both target and endogenous probes, 900 nM gyrase forward and reverse primers, and either 900 or 300 nM target primers (see Table S2 in the supplemental material) and were amended with nuclease-free water to a 40-μl volume. Ten microliters cDNA (0.4 ng/ml) or nuclease water was added. The PCR protocol was executed as follows: 50°C for 2 min and 98°C for 10 min, followed by 40 cycles of 95°C for 15 s and 60°C for 1 min on an Applied Biosystems sequence detection system 7300.

TABLE 3 Genomic coordinates of unannotated ORFs in the magnetosome island

ORF ID[a]	Genomic start site	Genomic termination site	Predicted function
R1-1	999169	999474	Conserved hypothetical in *Magnetospirillum gryphiswaldense* MSR-1
R1-2	1000521	1000664	PAS domain
R1-3	1000624	1001148	Amb0942; transposase/integrase
R2-1	1012739	1013047	Hypothetical
R2-3	1012526	1012876	Hypothetical
R6-1	1040560	1039265	CheY-like receiver
R6-2	1047290	1049650	Histidine kinase with PAS domain
R7-1	1050077	1060490	Transcriptional regulator
R7-2	1051136	1051576	Hemerythrin-like
R7-3	1053698	1052136	Hemerythrin-like plus receiver domain
R7-4	1054569	1053712	Hemerythrin-like plus receiver domain
R7-5	1054581	1055096	Hemerythrin-like
R8-1	1055440	1056360	Hypothetical
R8-2	1056558	1056959	Hypothetical
R8-3	1061118	1061810	Hypothetical
R8-4	1062536	1062712	Mms7
R8-5	1062783	1063055	Weak homology to peptidase sortase, TadE
R8-6	1063419	1063667	Weak homology to lipoprotein, thioredoxin
R10-1	1070046	1070339	Potential hydrogenase, ferric iron uptake regulator
R11-1	1075142	1075708	Hypothetical
R13-1	1092108	1092449	Hypothetical
R13-2	1091305	1090352	Hypothetical

[a] ORF identifier.

CtrA regulon prediction. CtrA regulons were predicted by using a position weight matrix (PWM), modeling the position-specific variability of CtrA binding motifs. The PWM was learned on experimentally defined CtrA targets in *C. crescentus* as described previously (6). Although the use of a heterologous model can be justified by the conservation of the binding motif in phylogenetically diverse members of the *Alphaproteobacteria*, we here decided to obtain a model trained on *M. magneticum* AMB-1, which could improve the predictions by taking into account the specific variability of DNA in this organism. Indeed, the 16mer corresponding to the CtrA binding motif comprises 9 positions that are well conserved and that give specificity to the matrix, but there are also 7 very variable positions, which in fact seem to model the background DNA, and thus it is specific to a given genome. To obtain the matrix, we used MDscan, an algorithm designed for enriched sequence motif identification (31). As input, we used the sequence from 500 nt upstream of ATG to 100 nt within the coding sequence of genes with a significant change of expression in the *ctrA* mutant and the full complement of intergenic sequences that is used by MDscan to derive a background model of DNA to weight the motif occurrences using a Markov model of the appropriate order. We obtained a sequence motif closely resembling the one known in *C. crescentus*, which was subsequently used to characterize the presence of CtrA binding motifs in the whole genome. The PWM was used to scan the *M. magneticum* AMB-1 genome, looking for occurrences of the CtrA binding motif in the region from 400 nt upstream of the translation start site of a gene to 100 nt

within the coding sequence. Occurrences of the motif were scored using the following formula:

$$S = \frac{1}{L}\sum_{j=1}^{L} 2\log_2 f_{ji}$$

where L is the length of the binding motif (in this case 16), and f_{ji} stands for the value located in the j^{th} row, i^{th} column of the PWM; the column is determined by the nucleotide found at the j^{th} position of the motif. This score is related to information theory and indeed represents the information content of the motif given the PWM. When scanning an entire genome and assigning a score to every overlapping L-mer, the distribution of scores follow a normal distribution (6), so that the scores can be transformed in Z scores to collect only those significant at a given threshold.

Enrichment analysis of CtrA regulon. Once a threshold was established for assigning a gene to the CtrA regulon on the basis of the Z score of the binding motif it owns upstream, we calculated whether there is some bias in the functional categories belonging to the regulon. We measured the enrichment of the regulon by means of 10,000 random sampling simulations in the genome. These results should be taken with caution, since this analysis simply reveals if the positive samples contain more genes of a given category than the average random samples, which is different from the effect of the regulator on the functional category, since indirect regulations can amplify the scope of a regulator with respect to its direct targets.

Transmission electron microscopy. For transmission electron microscopy (TEM) characterization, strains were grown under microaerobic conditions to an OD_{400} of ~0.2, and 1 ml of cells were centrifuged and resuspended in ~10 μl of MG medium. The cells were adsorbed onto 400-mesh copper grids (Ted Pella Inc.), and the grids were analyzed as described previously (36).

Phylogenetic analysis. Orthologous sequences were retrieved using the bidirectional best-hit criterion, whereby orthology relationships were established between proteins occurring reciprocal first BLAST hits. Orthologous sets for the universal proteins were further refined on the basis of a preliminary phylogenetic analysis to remove deviant proteins placed in unexpected phylogenetic positions with respect to known taxonomic relationships between organisms in the data set. Evolutionary analyses were performed using tools in the Mega 5 software program (51), and all alignments were obtained with the program Muscle (12).

To build the tree of universal sequences (see Fig. S6 in the supplemental material), which we use as a proxy for the species tree, we used the maximum-likelihood method (53) and a multialignment containing eight concatenated universal proteins. The proteins used were FusA, IleS, LepA, LeuS, PyrG, RecA, RecG, and RplB, which were identified as useful molecular markers (42). We also generated a phylogenetic tree of alphaproteobacteria based on CtrA sequences (see Fig. S7 in the supplemental material). The percentages of replicate trees in which the associated taxa clustered together in the bootstrap test (50 replicates) are shown next to the branches, whose lengths correspond to evolutionary distances between sequences computed using the JTT matrix-based method (22). The units expressed are the number of amino acid substitutions per site. The rate variation among sites was taken into account with a discrete gamma distribution (shape parameter = 1.3; 4 categories of rates). The analyses involved 47 amino acid sequences for both the universal and CtrA trees. All positions containing gaps and missing data were eliminated, giving a total of 2,188 positions for the universal and 182 for the CtrA final data sets.

A smaller CtrA tree, shown in Fig. 5, was built by including only those species of alphaproteobacteria in which the role of CtrA had been experimentally investigated, and it maintains the relative position of those species with respect to the complete tree. The bootstrap consensus tree inferred from 50 replicates (13) is taken to represent the evolutionary history of the taxa analyzed (13). Branches corresponding to partitions reproduced in less than 50% of bootstrap replicates are collapsed. The percentages of replicate trees in which the associated taxa clustered together in the bootstrap test (50 replicates) are shown next to the branches (13). An initial tree(s) for the heuristic search was obtained automatically as follows. When the number of common sites was <100 or less than one-fourth of the total number of sites, the maximum-parsimony method was used; otherwise, the neighbor-joining (BIONJ) method with maximum composite likelihood (MCL) distance matrix was used. A discrete gamma distribution was used to model evolutionary rate differences among sites (3 categories [+*G*, parameter = 0.9031]). The rate variation model allowed for some sites to be evolutionarily invariable ([+*I*], 12.9413% sites). The tree is drawn to scale, with each branch length measured in number of substitutions per site. The analysis involved 9 amino acid sequences, with a total of 231 positions in the final data set.

Microarray data accession number. Microarray results obtained in this work are available in the NCBI GEO database under the accession number GSE35625.

RESULTS

CtrA is not essential for viability or progression of the AMB-1 cell cycle. Components of the CtrA signal transduction pathway, essential for cell viability and progression of the *Caulobacter crescentus* cell cycle, are conserved throughout the *Alphaproteobacteria* (6). A search of the AMB-1 genome revealed the presence of homologs not only of *ctrA* (*amb0629*) but also of its negative regulator *divK* (*amb3750*), histidine kinase partner *cckA* (*amb0620*), and phosphotransferase gene *chpT* (*amb0327*). We generated nonpolar deletions of the AMB-1 homologs of *ctrA* and *divK* and found that the deletion strains were viable. Triplicate wild-type and Δ*ctrA* mutant strains were assayed for overall growth, as well as the ability to align in an external magnetic field, as determined through a spectrophotometric assay represented by the coefficient of magnetism (Cmag). In all stages of growth, the Δ*ctrA* mutant behaved identically to the wild type, both in growth characteristics and in acquisition of magnetism (Fig. 1A, C, and D). The slight decrease in Cmag in both wild-type and Δ*ctrA* strains around 15 h could be attributed to cell division and thus segregation of existing magnetosome chains to daughter cells prior to the synthesis of new magnetosomes which follows the depletion of oxygen in the culture tubes.

To determine whether any aspect of the cell division cycle was affected by the loss of CtrA, we synchronized populations of AMB-1, released cells into fresh growth medium, and visually monitored cell cycle progression. Previous studies investigating the role of the cell cycle in magnetosome formation in AMB-1 have relied on lengthy repeated cold treatments to synchronize cells (44, 56); in this work, density gradient centrifugation was used as a potentially less disruptive method to rapidly obtain synchronous populations of both wild-type and Δ*ctrA* strains. Briefly, exponential-phase cells are harvested and layered on a preformed density gradient of 50% Percoll in conical tubes. Upon subsequent centrifugation, AMB-1 cells are separated according to size as confirmed by light microscopy. Small, newly divided cells, concentrated at the top of the gradient, are harvested by pipetting and used to inoculate fresh cultures of AMB-1. Synchronization of resulting cultures was assessed through visual cell counts. Wild-type cultures maintain relatively constant cell numbers throughout the 4-h growth period, after which point the population doubles in size. AMB-1 cultures remain synchronized throughout two doubling periods. In triplicate synchronization experiments, the Δ*ctrA* strain also exhibited synchronous growth with a 4-h doubling period when subjected to the same treatment as wild-type AMB-1 (Fig. 1B; see also Fig. S1 in the supplemental material).

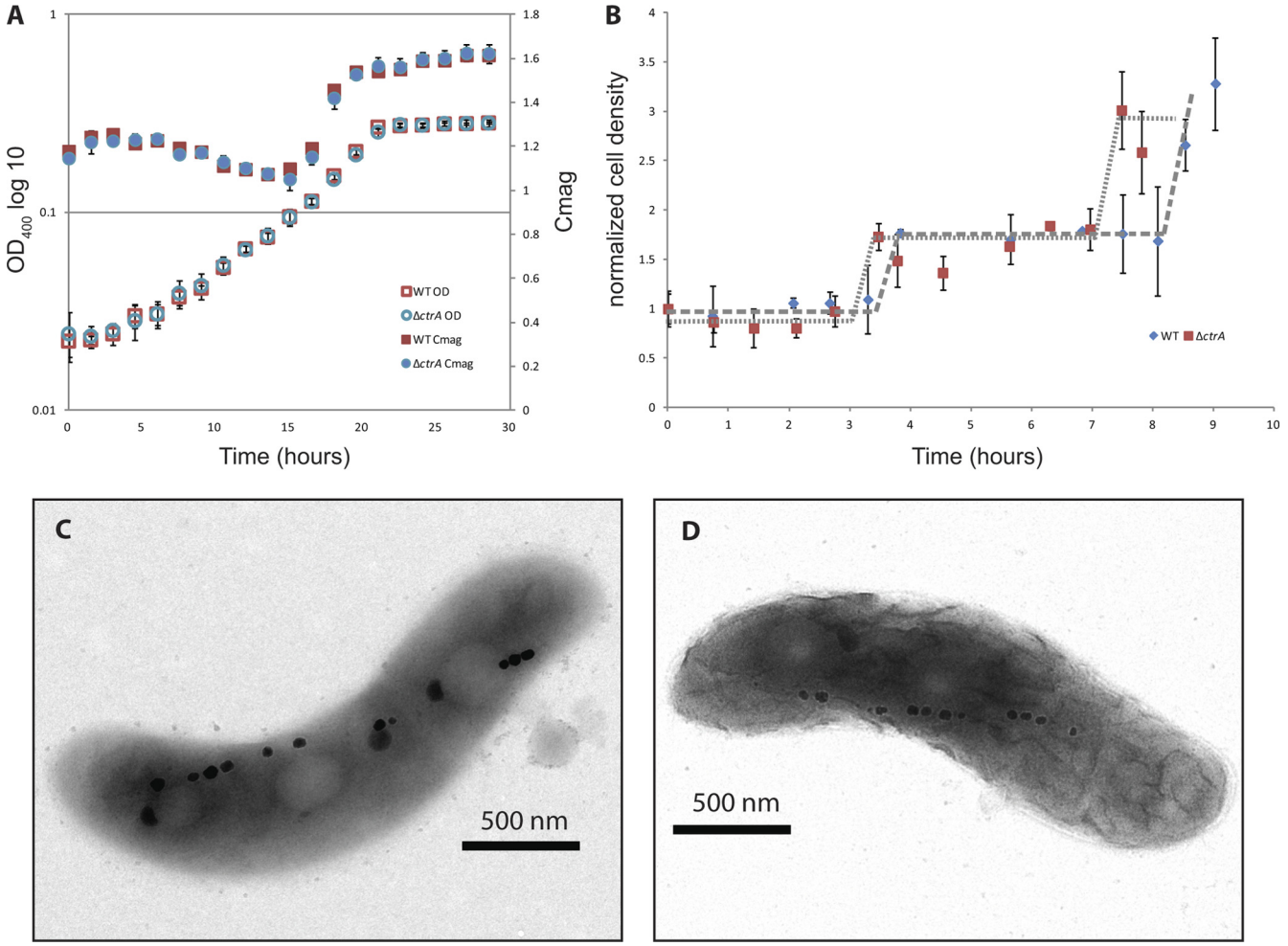

FIG 1 CtrA is conserved but not essential for viability or growth in AMB-1. (A) Growth (OD_{400}) and magnetism (Cmag) of wild-type and *ctrA* deletion strains. The ability to turn in a magnetic field was assessed spectrophotometrically as described previously (26). A Cmag of 1 indicates a nonmagnetic culture. (B) Synchronization of wild-type and Δ*ctrA* AMB-1 via density gradient centrifugation was assessed through visual cell counts of cells released in fresh MG medium. Shown are representative data from single synchronies of each strain. Triplicate biological replicates were performed, and data from these experiments are included in Fig. S1 in the supplemental material. Error bars reflect errors in cell counting from triplicate cell counts at each time point. (C and D) Transmission electron micrograph of a representative wild-type (C) or Δ*ctrA* (D) strain, highlighting the presence of magnetosome chains containing cubo-octahedral crystals.

The timing offset of the initial cell doublings between wild-type and Δ*ctrA* strains reflects variation between experiments in the accuracy of harvesting the most newly divided cells from the uppermost Percoll layer rather than a growth rate difference, supported by the results in Fig. 1A. These results suggest that CtrA is not essential for AMB-1 viability, nor does it play a prominent role in the progression of the cell cycle.

CtrA and DivK regulate motility in AMB-1. During mutant characterization, it was observed that on average 20% (and up to 30%) of Δ*divK* mutant cells exhibited constitutive motility. This is unlike the motility behavior of wild-type AMB-1, which upon isolation and under standard laboratory conditions is nonmotile (less than 1% of exponential-phase cells swim) (32). In contrast to the minimal wild-type swimming activity, a spontaneous loss of the magnetosome island (MAI) renders the cells not only incapable of producing magnetosomes but also motile, such that 100% of the cells are swimming in liquid culture. Further, wild-type AMB-1 rarely produces flagella, while ΔMAI cells are consistently flagellated (see Fig. S2 in the supplemental material). Potentially, the MAI encodes a negative regulator of motility, which, when lost, renders the cells incapable of regulating their swimming behavior. While a *divK* deletion does not phenocopy a deletion of the MAI, the phenotype was intriguing, since *ctrA* has been well characterized as a class I flagellar biosynthesis gene for its regulation of flagellar gene expression in *C. crescentus* and a regulator of motility in a number of other alphaproteobacteria (6, 29, 38).

To determine whether CtrA could indeed act as an upstream regulator of flagellar biosynthesis in AMB-1 and its relation to factors controlling motility in the MAI, we generated a deletion of *ctrA* in the hypermotile ΔMAI background. The double mutant was completely nonmotile, suggesting a role for the CtrA pathway in motility in AMB-1 and furthermore suggesting that its regulation of motility is downstream of factors in the MAI (Fig. 2A). Expression of CtrA from a plasmid was sufficient to restore motility to the double-mutant strain.

Putative phosphorylation of CtrA is essential for motility. CtrA belongs to the OmpR subfamily of response regulators and is characterized by an additional C-terminal DNA binding domain

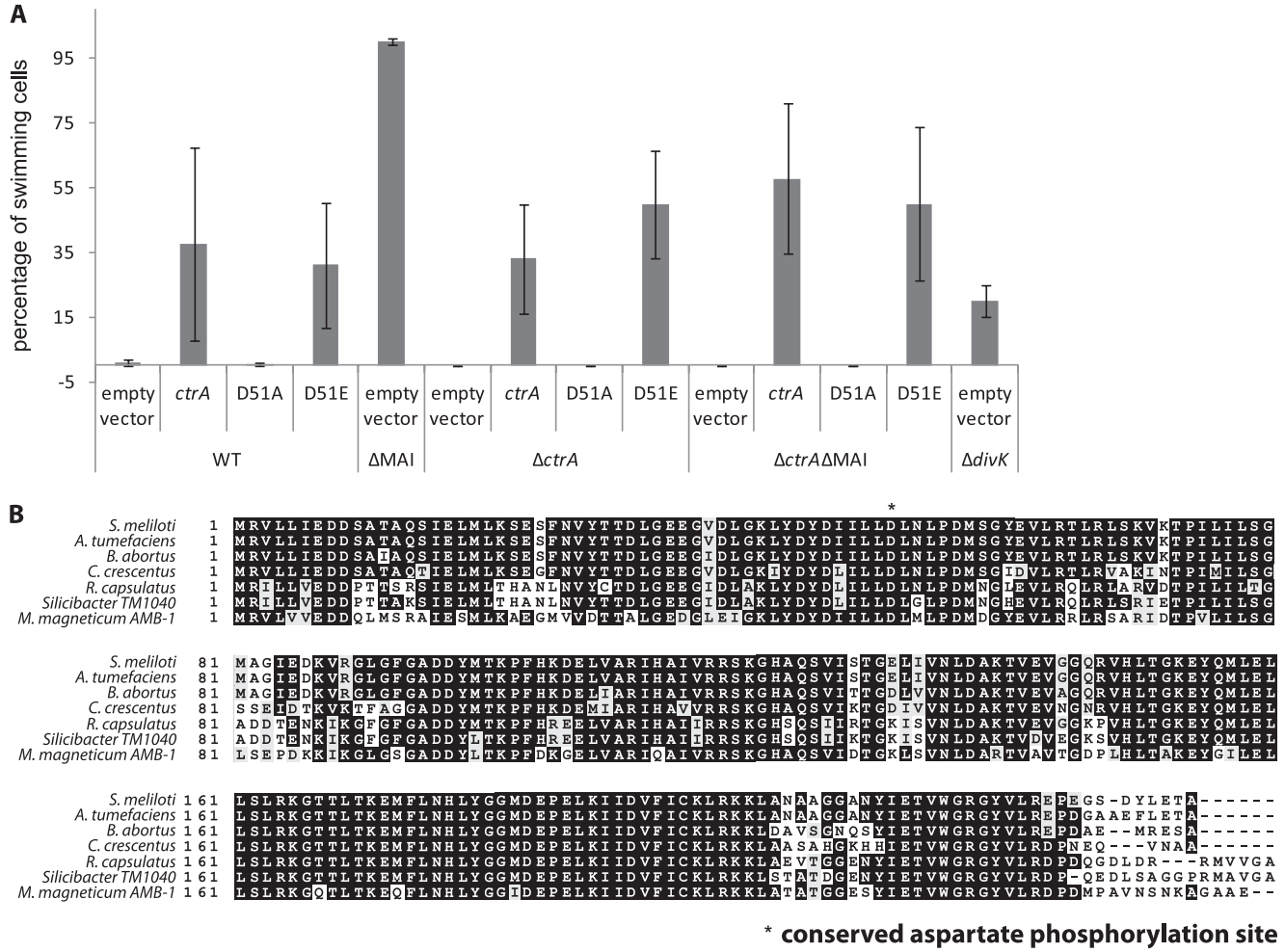

FIG 2 (A) Percentages of motile cells in wild-type AMB-1 and mutant strains as assessed visually using light microscopy. Error bars represent standard errors from at least 10 biological replicates for each strain, grown in separate experiments. (B) Multiple sequence alignment of CtrA homologs from alphaproteobacteria in which the role of CtrA has been investigated (ClustalW). The phosphorylation site, position D51 in *C. crescentus*, is conserved in all species.

(38). Members of this family possess a conserved aspartate residue inside the receiver domain, phosphorylation of which alters activity. In *C. crescentus*, phosphorylation of CtrA occurs exclusively at position D51 and is essential for cell viability (38). As such, phosphorylation is tightly regulated, with the response regulator DivK inhibiting phosphate flow to CtrA (3). Replacing the conserved aspartate residue in CtrA with a glutamate prohibits actual phosphorylation of the protein yet mimics the active, phosphorylated state and provides essential cell activities (10, 47). This critical aspartate residue is conserved in the AMB-1 homolog of CtrA (Fig. 2B). The motility phenotype of the *divK* deletion, ostensibly removing a negative regulator of CtrA in the signal transduction pathway, suggests that CtrA's activity in AMB-1 is controlled in a manner similar to that in *C. crescentus*.

To determine whether potential phosphorylation of CtrA is involved in regulation of motility in AMB-1, we complemented the WT, Δ*ctrA*, and Δ*ctrA* ΔMAI strains with alleles mimicking the phosphorylated and active (D51E) and unphosphorylatable and inactive (D51A) versions of CtrA. Mutating the conserved aspartate residue to glutamate (CtrA D51E) yielded an increase in motile cells above the levels achieved with wild-type CtrA in the Δ*ctrA* background (50% against 33%, respectively) (Fig. 2A). CtrA D51E expressed in the Δ*ctrA* ΔMAI strain did not increase the level of swimming beyond that of wild-type CtrA (50% against 57%, respectively), possibly indicating that although the CtrA D51E allele is sufficient to overcome the negative regulation of motility from the MAI, expression of wild-type CtrA is better able to complement the Δ*ctrA* ΔMAI strain. In both complementation experiments, expression from the vector and plasmid maintenance may explain the lack of fully restored motility in these strains.

In contrast to complementation experiments with wild-type CtrA and CtrA D51E alleles, no motile cells were ever observed when expressing CtrA D51A from the identical construct. At this time, we cannot exclude the possibility that the CtrA D51A protein is less stable than the wild type or the CtrA D51E allele, thus explaining its inability to complement the loss of *ctrA*. It is important to note that the transcript levels for all three versions of *ctrA* are similar in these experiments (see the microarray data below). Moreover, given the known behavior of CtrA in other systems, we believe that these results suggest that the phosphorylation state of CtrA is essential for motility in AMB-1 and that swimming behav-

ior observed in the *divK* deletion strain potentially stems from an increased population of phosphorylated and active CtrA.

CtrA regulon in AMB-1 is distinct from that of *Caulobacter*. In alphaproteobacterial species where CtrA is not essential for viability, such as *R. capsulatus*, *R. centenum*, and *Silicibacter* sp. TM1040 (4, 27, 34, 46), CtrA still appears to regulate flagellar motility. In AMB-1, CtrA is also not essential, does not appear to play a role in the formation of magnetosome organelles, and seems to be involved in the regulation of motility. To ascertain the role of CtrA more specifically in motility and to learn about its regulon in a bacterium in which it is not essential for viability, we used microarrays to probe global gene expression patterns when different alleles of CtrA were expressed.

Microarrays were designed using the published AMB-1 genome (GenBank accession no. AP007255). Each array contained duplicated genomic probe sets, with seven probes per gene. Additional probe sets detecting the expression of unannotated ORFs in the magnetosome island were designed; these 22 ORFs were predicted by ORF Finder (Table 3). To identify the CtrA regulon in AMB-1, we analyzed cDNA reverse transcribed from RNA extracted from triplicate biological replicates of wild-type AMB-1, the Δ*ctrA* and Δ*divK* mutants, and the Δ*ctrA* mutant complemented with CtrA D51E, CtrA D51A, or an empty expression vector (Δ*ctrA* + CtrA D51E, Δ*ctrA* + CtrA D51E, and Δ*ctrA* + empty vector). Because the *ctrA* deletion mutant behaves phenotypically like wild-type AMB-1 under the conditions tested, we relied on the expression of mutant CtrA alleles to identify genes regulated, positively and negatively, by CtrA. Genes whose expression increased at least 1.5-fold for the Δ*ctrA* + CtrA D51E strain relative to that for the Δ*ctrA* + CtrA D51A and Δ*ctrA* + empty vector strains were considered in this study to be upregulated by CtrA (Fig. 3A; see also Fig. S7 in the supplemental material). This positive CtrA regulon contains 283 genes, with 103 genes having at least 2-fold increases in gene expression.

Of the 283 genes comprising the potential CtrA regulon in AMB-1, 14 were identified with roles in flagellum biosynthesis, 7 of which are in a putative operon (*amb0498* to *amb0506*) (Fig. 3B). These genes encode proteins which comprise the motor switch and hook and basal body components of the flagella. Eleven of those fourteen flagellar biosynthesis genes were similarly upregulated in the *divK* deletion strain. The flagellin-like genes *amb1999* and *amb0684* were expressed at high and moderate levels, respectively, in all genetic backgrounds and thus do not appear to account for the lack of motility in wild-type AMB-1. Rather, the production of the basal aspects of the flagella appears to be the limiting factor in determining the ability of AMB-1 to swim. The increased expression of flagellar biosynthesis genes in the Δ*divK* strain and cells expressing the active-mimic allele CtrA D51E suggests that phosphorylated CtrA is necessary for the transcription of these genes, either directly or indirectly, and supports the observed motility phenotypes. Microarray gene expression results for two genes, *amb2833* and *amb0504*, which encode a hypothetical protein and the flagellar hook protein FlgE, respectively, were confirmed by quantitative RT-PCR (see Fig. S3 in the supplemental material).

Other members of the potential CtrA regulon which could contribute to the regulation of swimming behavior of AMB-1 include four transcriptional regulators (encoded by *amb0659*, *amb1405*, *amb2069*, and *amb2080*), two histidine kinases (encoded by *amb1336* and *amb2644*), and five additional response regulators (encoded by *amb0348*, *amb0848*, *amb2829*, *amb3405*, and *amb4301*). While upregulation of several flagellar biosynthetic gene clusters was observed, it is possible that this gene expression pattern is due to a downstream effect of the CtrA D51E allele and not to direct transcriptional control by CtrA itself. Bioinformatic prediction of CtrA binding sites in AMB-1, discussed subsequently, supports the hypothesis that the CtrA regulon as identified by microarray contains several indirect targets, possibly a result of downstream regulatory and transcription factors.

Beyond genes with putative motility and regulatory functions, genes encoding metabolic and transport factors were highly enriched in the identified CtrA regulon (Fig. 4A). This class of genes includes several ABC-type transporters, electron transfer flavoproteins, NADH oxidoreductases, and factors involved in nitrogen metabolism. In sum, these genes constitute 57 of the 283 genes in the potential CtrA regulon. Under standard laboratory conditions, no growth advantage or disadvantage has been detected for cells expressing CtrA D51E (data not shown), nor does the growth of the Δ*ctrA* mutant deviate from wild-type growth (Fig. 1). However, these results do not preclude the possibility of growth effects under different growth conditions.

Compared to the positive CtrA regulon, fewer genes (169 in sum) were downregulated more than 1.5-fold in the Δ*ctrA* + CtrA D51E strain than in both the Δ*ctrA* + CtrA D51A strain and the empty-vector control (see Fig. S4 and S8 in the supplemental material); 31 of these were downregulated more than 2-fold. The majority of these genes encode hypothetical proteins, although among them are genes encoding additional metabolic and redox proteins and 18 putative regulatory proteins. Again, the only deviation in phenotype observed under standard laboratory conditions between the Δ*ctrA* + CtrA D51E strain and the Δ*ctrA* strain was increased motility, so the effects of downregulating these 169 genes are unknown. Given the number of regulatory genes affected both positively and negatively by the expression of CtrA D51E, it is likely that many of the components of the putative regulon are not direct targets of CtrA.

In *C. crescentus*, CtrA has been shown to regulate genes cotranscribed in operons or divergently transcribed from a shared promoter region (29). A search in AMB-1 revealed that 81 genes upregulated by the expression of CtrA D51E are potentially transcribed in operons, and 4 are potentially divergently transcribed from a shared regulatory region. These gene clusters include genes encoding flagella biosynthesis, cytochrome synthesis, nitrogen fixation, and sulfite reduction functions. Similarly, repressed expression of 30 genes is potentially due to transcription from 14 shared promoters, while an additional 9 genes are potentially divergently expressed from 4 shared regulatory regions.

Of particular note is the paucity of cell cycle control genes found to be regulated by the expression of CtrA D51E. In *C. crescentus*, the CtrA regulon is known to directly control the transcription of such factors as *ftsZ*, *ftsW*, *dnaA*, and *ccrM* (24, 29, 30). Of these factors, only the AMB-1 homolog of the essential *C. crescentus* methyltransferase CcrM (*amb3988*) was upregulated by expression of CtrA D51E, but since a *ctrA* deletion mutant was viable, *ccrM* is also unlikely to be essential in AMB-1. Additionally, our microarray data suggest that *ccrM* is expressed in the Δ*ctrA* mutant but that its expression increases upon the introduction of the CtrA D51E allele. Because homologs of other critical cell cycle genes were not identified in

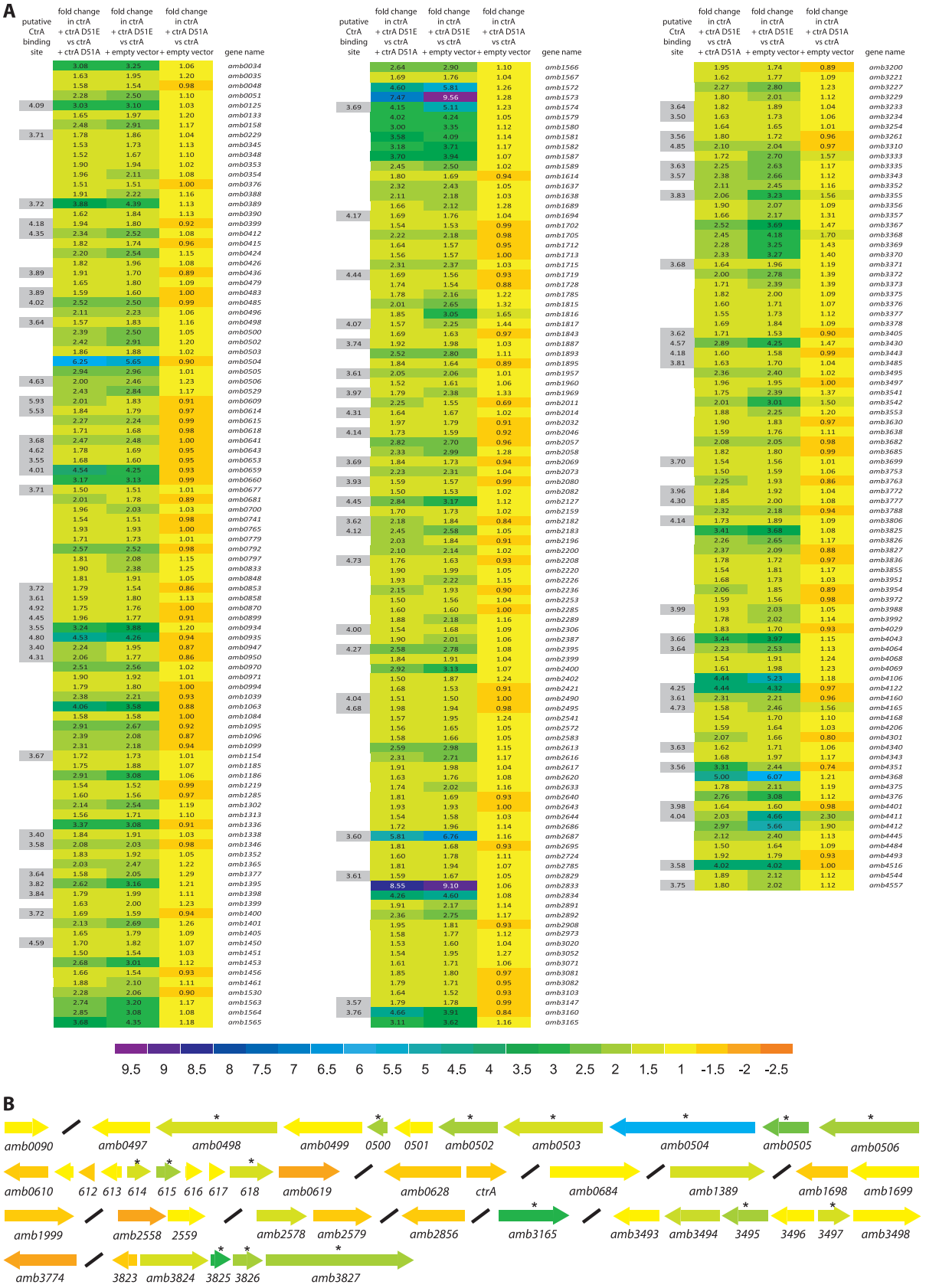

FIG 3 (A) Two hundred eighty-three genes were upregulated at least 1.5-fold in cells with *ctrA* deletions expressing CtrA D51E compared to those expressing CtrA D51A and the empty vector control. These genes are depicted in genomic order and are colored according to their fold change in expression in the Δ*ctrA* mutant complemented with the CtrA D51E allele versus the CtrA D51A allele. The leftmost column denotes the presence of a putative CtrA binding site, using a Z-score cutoff of 3.40. (B) Genomic context of flagellar biosynthesis genes in AMB-1. Genes are colored as in panel A; slashes indicate gaps between flagellar biosynthesis genes and gene clusters. Of the 46 genes potentially involved in flagellar biosynthesis, 17 were upregulated at least 1.5-fold in *ctrA* deletions expression CtrA D51E rather than CtrA D51A and the empty vector control; those genes are indicated by asterisks.

A **Frequency of COG categories in the microarray CtrA regulon**

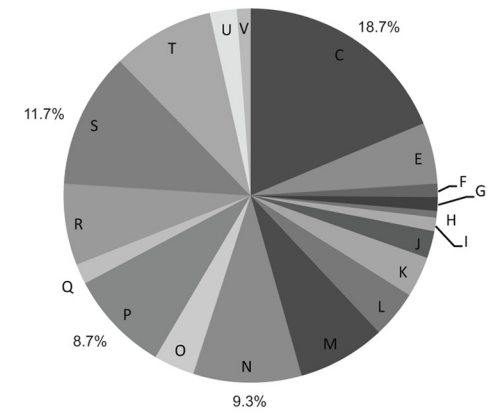

Frequency of COG categories in the AMB-1 genome

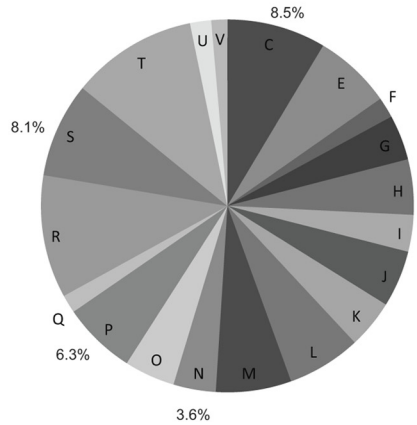

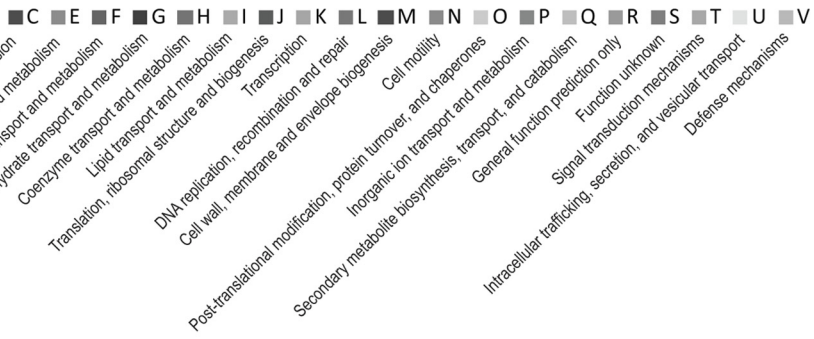

B

	COG categories	P-value	# genes in genome	# genes with CtrA motif
-	Not Assigned	0.0193	1432	34
P	Inorganic ion transport and metabolism	0.02	197	8
T	Signal transduction mechanisms	0.0608	338	10
K	Transcription	0.0736	130	5
N	Cell motility	0.5916	114	2
S	Function unknow n	0.6518	255	4
L	Replication, recombination and repair	0.6795	198	3
E	Amino acid transport and metabolism	0.7027	208	3
J	Translation, ribosomal structure and biogenesis	0.7392	152	2
M	Cell w all/membrane/envelope biogenesis	0.8705	203	2
O	Posttranslational modification, protein turnover, chaperones	0.9045	136	1
R	General function prediction only	0.9291	330	3
C	Energy production and conversion	0.9499	266	2
A	RNA processing and modification	1	0	0
B	Chromatin structure and dynamics	1	0	0
D	Cell cycle control, cell division, chromosome partitioning	1	27	0
Y	Nuclear structure	1	0	0
V	Defense mechanisms	1	43	0
Z	Cytoskeleton	1	0	0
W	Extracellular structures	1	0	0
U	Intracellular trafficking, secretion, and vesicular transport	1	57	0
G	Carbohydrate transport and metabolism	1	121	0
F	Nucleotide transport and metabolism	1	55	0
H	Coenzyme transport and metabolism	1	149	0
I	Lipid transport and metabolism	1	99	0
Q	Secondary metabolites biosynthesis, transport and catabolism	1	49	0

FIG 4 (A) Comparison of COG representation frequencies in genes positively regulated by CtrA D51E and in the entire AMB-1 genome. The CtrA regulon, as identified by microarray analysis, is enriched in functional categories C (energy production and conversion), N (cell motility), P (inorganic ion transport and metabolism), and S (hypothetical proteins). (B) Genes of unknown function and those predicted to encode proteins involved in inorganic ion transport and metabolism were enriched relative to the AMB-1 genome in upstream putative CtrA binding motifs ($P < 0.05$). Genes with predicted signal transduction and transcription functions were slightly enriched in such putative CtrA binding motifs ($P < 0.1$).

our data set, the progression of the cell cycle is potentially decoupled from CtrA, suggested by our viability and synchronization data. The regulation of these factors and the progression of the AMB-1 cell cycle remain elusive.

CtrA regulon in AMB-1 is enriched in potential CtrA binding sites. Because the putative CtrA regulon as predicted by microarray results contained several genes encoding regulatory proteins, it is possible that some gene expression changes are due to indirect effects of CtrA D51E expression. To more precisely determine the potential CtrA regulon in AMB-1, we modeled the AMB-1 CtrA binding motif as a probability matrix as explained in Materials and Methods. Genes identified as part of the putative CtrA regulon by microarray analysis were scanned across a −500 to +100 window relative to the start site and assigned Z scores according to the probability that their upstream sequence contains occurrences of CtrA binding with respect to the background DNA. The consensus AMB-1 CtrA binding motif was determined to be TTAA(CG NANNT)TAA[T/A]C. This motif was then used to scan the entire AMB-1 genome for putative CtrA binding sites.

Using a threshold of 4 for the Z score per CtrA motif occurrence, the CtrA regulon as defined by the gene expression results is enriched in the potential CtrA binding sites relative to the rest of the AMB-1 genome ($P = 0.0018$). Genes possessing a significant CtrA binding motif include *amb0614* and *amb0506*, which encode flagellar basal body and hook-length regulatory proteins, respectively (Fig. 3A). While there remains a significant proportion of the proposed CtrA regulon which does not contain detectable CtrA binding sites by homology to the *C. crescentus* motif, these genes could be under indirect CtrA control, since several proteins of putative regulatory function were identified as being both upregulated by CtrA D51E and possessing a possible upstream CtrA binding motif (*amb2014*, *amb0659*, *amb2080*, *amb2069*, *amb3405*, *amb2829*, *amb3261*, *amb2643*, and *amb0848*). False negatives are also present in the predictions, because (i) we applied a necessary but arbitrary threshold to include a motif occurrence, and (ii) transcription factor binding motifs are intrinsically variable, which is at the basis of the difficulties in reconstructing gene regulatory networks from sequence alone. Autoregulation of CtrA is a feature well characterized in *C. crescentus* (11) and has also been suggested for *S. meliloti* CtrA based on the presence of five CtrA-binding motifs identified in its own promoter (1). A low-score motif was detected upstream of CtrA itself in AMB-1, which indicates possible autoregulation as well (data not shown).

Random sampling of the AMB-1 genome for genes carrying the CtrA motif and a subsequent comparison of the representation of cluster of orthologous gene (COG) categories in this group of genes against the genomic COG distribution (6) reveal that targets of CtrA are enriched in genes with no assigned function, inorganic ion transport and metabolism, and to a lesser extent signal transduction mechanisms and transcription (Fig. 4B). The modest enrichment in genes with putative roles in transcription could suggest that the effect of CtrA is mediated by specific regulators. It should be noticed that enrichment analyses in general provide a biased estimate of the importance of CtrA for regulating a given functional category. Indeed, it has been shown that CtrA is crucial for motility in AMB-1, while the category is not enriched. For motility, this depends on the functional role of the targets and their position in a hierarchical network of events. One of the targets we obtained, *amb0614* (*flgB*), has been classified in *C. crescentus* as a class II flagellar gene, demonstrating that despite the small number of genes directly regulated by CtrA, the influence of the regulator is important.

While the predictions made regarding the identity and role of the CtrA binding motifs in AMB-1 has not yet been confirmed by *in vitro* or *in vivo* DNA binding assays, the detected motif is quite similar to that characterized in *C. crescentus*, and its enrichment upstream of genes in the CtrA regulon is suggestive of direct CtrA control.

Regulation of magnetosome island genes by CtrA. Based on gene expression and computational data sets, genes in the MAI are among those in the CtrA regulon in AMB-1. Three genes in particular were highly upregulated by the expression of CtrA D51E with respect to CtrA D51A and empty vector control strains. These genes are *amb0934*, *amb0935*, and *amb0970*, whose expression levels increased 3.2-fold, 4.5-fold, and 2.5-fold, respectively, between CtrA D51E-expressing and CtrA D51A-expressing strains. None of these genes has an upstream predicted CtrA binding site, and no phenotype was detected in a deletion of a region of the MAI encompassing both *amb0934* and *amb0935* (36). However, a deletion of *amb0970*, which encodes the magnetosome membrane protein MamP, results in the biomineralization of only one or two very large magnetite crystals per cell (36). Because no biomineralization defect was detected in the Δ*ctrA* strain complemented with CtrA D51E compared to the wild type, this suggests that the degree of overexpression of *mamP* in the microarray experiments does not adversely affect magnetosome formation (data not shown). Additional MAI genes were upregulated by the expression of CtrA D51E; these include three potentially unannotated open reading frames. As mentioned above, our microarray contains seven 60mer probes designed against open reading frames not present in the annotated AMB-1 genome but which are predicted by ORF Finder. Two of these genes are predicted hypothetical ORFs in region 2 of the MAI (R2-1 and R2-2), and a third is a predicted hypothetical ORF in region 8 of the MAI (R8-1). Of further note was the slight overexpression of *amb0994*, encoding a predicted methyl-accepting chemotaxis protein, which was recently shown to form polar clusters in AMB-1 and to interact with MamK, an actin-like protein involved in the chain organization of magnetosomes (37). Although *amb0994* was not as significantly overexpressed relative to other genes in the CtrA regulon (1.74-fold), its promoter region does possess strong homology to a CtrA binding site, suggesting direct CtrA control. Altogether, these results indicate that CtrA-dependent changes in the expression level of some MAI genes do not lead to discernible disruptions in magnetosome formation or magnetotaxis.

Phylogenetic analysis of CtrA homologs in alphaproteobacteria. Phylogenetic trees constructed from concatenated sequences of universal proteins and from CtrA sequences retrieved across the *Alphaproteobacteria* are mostly congruous, indicating a lack of horizontal transfer of CtrA homologs within the group (see Fig. S5 and S6 in the supplemental material). The most notably divergent CtrA sequence from *Acidiphilium cryptum* does not have an obvious conserved aspartate phosphorylation site. Integrating a condensed phylogenetic tree of CtrA sequences, which highlights only those species of alphaproteobacteria in which the biological roles of CtrA have been experimentally investigated, with the associated experimental results allows us to place a divergence event, denoted by a star, beyond which point one CtrA lineage acquired an essential role in its hosts (Fig. 5). Mapping observed functions of CtrA onto this condensed tree further sug-

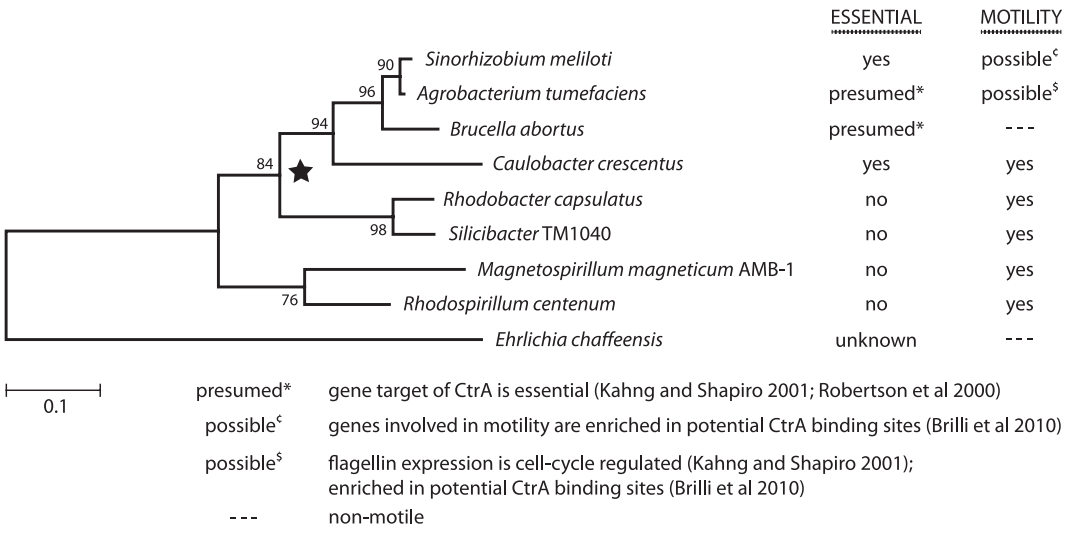

FIG 5 Phylogenetic tree depicting the evolutionary relationships among CtrA homologs from alphaproteobacteria in which the role of CtrA has been investigated. When mapping the role(s) of CtrA onto the phylogenetic tree, a branch point (star) between organisms in which CtrA is essential or presumed to be essential for viability and those in which CtrA is dispensable is suggested. Species which evolved from one lineage (*S. meliloti*, *A. tumefaciens*, *B. abortus*, and *C. crescentus*) have essential or presumed-essential functions for CtrA. Species evolved from the alternate lineage and more ancestral divergent lineages (*R. capsulatus*, *Silicibacter*, *M. magneticum*, and *R. centenum*) lack an essential role for CtrA. In each of the above species, CtrA plays a role in the regulation of motility. Excepting the nonmotile *B. abortus*, *A. tumefaciens* and *S. meliloti* encode motility genes with potential upstream CtrA binding sites (6), and further, flagellin expression in *A. tumefaciens* is cell cycle regulated (23). CtrA regulates the stress response in the intracellular pathogen *Ehrlichia chaffeensis*, but its roles in viability and motility are unknown (8).

gests an ancestral role in motility for CtrA in the *Alphaproteobacteria*.

DISCUSSION

Regulation of motility in AMB-1. In this study, we have shown that CtrA in AMB-1 is not essential for cell viability, nor does its loss induce observable cell division defects. Further, we have shown that the Δ*ctrA* mutant is indistinguishable from wild-type AMB-1 in its ability to align in a magnetic field throughout its growth. A comparison of wild-type AMB-1 with Δ*ctrA* mutants provides only a faint hint of the role of CtrA, since the occasionally swimming wild-type cells are never observed in the Δ*ctrA* strain. However, since a strain with a deletion of *ctrA* in the hypermotile ΔMAI genetic background is nonmotile, this work suggests a terminal role for CtrA in the regulation of motility in AMB-1. The inability of the Δ*ctrA* ΔMAI strain to swim suggests that CtrA itself is genetically downstream of factors regulating motility encoded in the MAI. In addition, complementing a *ctrA* deletion with CtrA D51E renders half of the cells motile, thus overcoming inhibition from the MAI. The motility of the *divK* deletion strain further supports the model that phosphorylated CtrA is necessary for expression of flagellar biosynthesis genes and the swimming behavior of AMB-1 (Fig. 6).

However, the *divK* deletion achieved only 20% motility compared to that of the cells of the ΔMAI strain, 100% of which are motile. Thus, other regulatory factors are certain to play roles in the phosphorylation or stability of CtrA in AMB-1. These regulatory agents could be linked to the MAI or could be independent. The C terminus of CtrA in AMB-1 is highly divergent from that of CtrA in *C. crescentus* and does not possess an *ssrA*-like degradation tag, however, so regulation by ClpXP proteolysis seems unlikely (10, 41).

Magnetoaerotaxis. The ability to swim proves beneficial for aquatic microorganisms, since they can propel themselves through liquid medium to seek out environments most suited to their metabolic capabilities. Combining flagellar motility with chemotactic sensory and regulatory systems further enables bacteria to sample their current environment and either maintain or alter their trajectory based upon the chemicals sensed. Magnetotactic bacteria, such as *Magnetospirillum magneticum* sp. AMB-1, possess an additional directional sense, in that they can use their internal magnetosome chains to passively align with external magnetic fields. It has been proposed that such an alignment limits a three-dimensional search for optimal aquatic environments to one dimension, thus increasing the efficiency with which these organisms find microaerobic or anaerobic environments (48). This behavior is termed magnetoaerotaxis when alignment with magnetic fields is combined with an aerotactic search for low oxygen concentrations (14).

Most species of magnetotactic bacteria swim constitutively when grown in culture. Interestingly, we find that the vast majority of wild-type AMB-1 cells in culture are nonmotile. This is in stark contrast to other published studies (see reference 37 as an example) in which entire populations of AMB-1 cells were found to be swimming. It is possible that slight differences in growth medium components or environmental conditions account for the differences seen in these various studies. However, it is also likely that motile cells were selected for using a magnetically guided swimming-based procedure termed the "racetrack" assay. This is a common practice among some groups working with magnetotactic bacteria (55). In the case of AMB-1, such a procedure might select for genetic variants that would give rise to constitutively swimming strains. Finally, the swimming behavior observed in our lab precisely follows the first description of AMB-1 by Matsunaga et al. in 1991: "over 95% of magnetic cells were nonmotile during all stages of growth" (32).

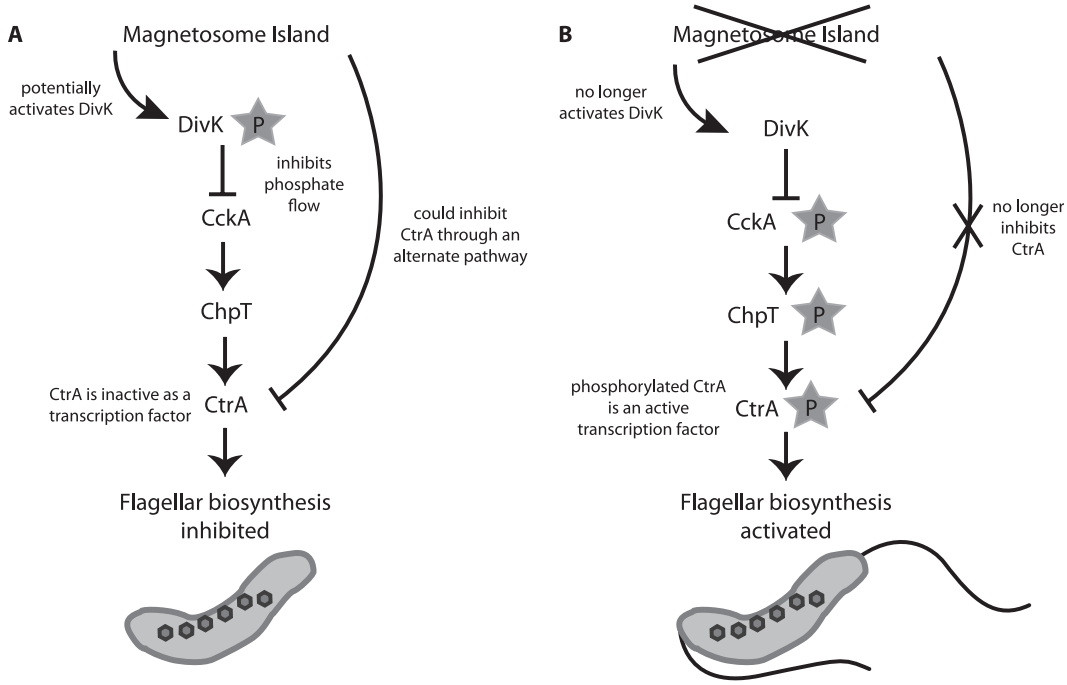

FIG 6 Model of the CtrA network and regulation of motility in AMB-1. We propose that CtrA is activated by phosphorylation through a pathway consistent with that in *C. crescentus*, whereby phosphate is transferred from CckA to CtrA via the phosphotransferase ChpT. Once it becomes phosphorylated, active CtrA promotes the transcription of flagellar biosynthesis genes. (A) In wild-type AMB-1, CtrA is deactivated by a factor or factors in the magnetosome island, either through its own repressor DivK or an alternative pathway. (B) In the magnetosome island deletion strain, repression of CtrA is lost and transcription of flagellar biosynthesis genes leads to active flagellum production and motility.

Given the current hypothesis explaining the evolutionary benefits of magnetosome chain formation, the lack of motility in AMB-1 is indeed surprising. Wild-type AMB-1 fails to swim even when challenged with increased or decreased iron or oxygen concentrations (unpublished results). Potentially, the isolation and current growth conditions are sufficient to satisfy the nutritional and energetic requirements of AMB-1, thus negating any reason to devote cellular energies toward building and rotating flagella. Still, the dramatic swimming behavior of the Δ*MAI* strain and the motility induced upon expression of CtrA D51E show that AMB-1 is indeed capable of swimming but that this behavior is repressed in wild-type cells. Given that magnetoaerotaxis is a defining characteristic of AMB-1, of which motility is a critical part, a means to regulate that motility could be evolutionarily advantageous. Understanding the mechanism by which factors in the MAI influence motility through the CtrA pathway will be fruitful progress in the field. Thus far, a genetic dissection of the MAI has not yielded mutants with increased motility like that seen in ΔMAI mutants, hinting at genetic redundancy or multiple layers of regulation within the MAI (36). As mentioned above, MB are commonly isolated using the "racetrack assay." Thus, it is possible that the isolation of these organisms has been biased toward specific species or genetic variants that are constitutive swimmers.

Role of CtrA in AMB-1. Beyond the motility phenotypes observed in the Δ*divK* and Δ*ctrA* ΔMAI strains, no additional phenotypic variations from the wild type were observed. CtrA does not appear to play an essential role in the viability or the cell division cycle of AMB-1. One of our initial questions was whether the CtrA pathway might play a role in the development or segregation of bacterial organelles, since it serves to direct flagella and stalk biogenesis in *C. crescentus*, as well as the production of gene transfer agent particles in *R. capsulatus* (27, 28). Again, we could detect no defect in magnetosome formation in the *ctrA* deletion or complemented strains either by the Cmag assay or by TEM. Interestingly, some MAI genes are constituents of the proposed CtrA regulon, as detected by microarray analysis of the Δ*ctrA* strain complemented with CtrA alleles mimicking either active or inactive forms of the protein. One such gene, *amb0970*, or *mamP*, was significantly upregulated when D51E was expressed relative to D51A or empty vector controls; it was shown previously that the loss of *mamP* has severe consequences for crystal number and size (36). Potentially, the transcriptional increases of *mamP* beyond wild-type levels are not sufficient for altering magnetite biomineralization.

Essential features of CtrA in *C. crescentus*, such as the regulation of DNA replication and cell division, fall outside the sphere of influence of CtrA in AMB-1. The coordination of these events with the segregation and division of the magnetosome chain remains elusive.

Divergent roles of CtrA in alphaproteobacteria. The common feature of the CtrA pathways in many alphaproteobacteria appears to be its role in motility and more specifically in flagellar biosynthesis. Genetic, gene expression, and promoter analyses in *C. crescentus*, *Rhodobacter capsulatus*, *Rhodospirillum centenum*, *Silicibacter* sp. TM1040, and now *M. magneticum* AMB-1 have shown the involvement of CtrA in the regulation of motility. In particular, phosphorylation of CtrA appears to be essential for this role. Expression of CtrA D51A in *R. centenum* is not sufficient to restore wild-type swarm behavior in a Δ*ctrA* mutant (4). While dependence on the phosphorylation state has not been established

for CtrA in *R. capsulatus*, gene expression analysis of a *ctrA* disruption mutant revealed that CtrA is primarily a positive regulator of genes in this organism and is required for expression of flagellar biosynthesis and chemotaxis genes (33). Despite the commonality of motility regulation by the CtrA regulatory pathway in these species, CtrA also takes on alternative, and sometimes essential, roles in each organism which carries the gene.

Analysis of the phylogenetic relationships among CtrA alleles from organisms in which its biological role has been investigated suggests that regulation of motility by CtrA is an ancestral trait (Fig. 5). A divergence event, noted with a star in Fig. 5, demarks a boundary between organisms in which CtrA has acquired an essential role from those in which CtrA retains control of motility and other, nonessential functions unique to its host. In *C. crescentus*, the essential role of CtrA in viability, as well as its role in flagellar biosynthesis, has been well characterized. While a direct link between CtrA and motility has not been established in *A. tumefaciens*, motility and flagellin gene expression vary across the cell cycle, progression of which is hypothesized to rely on CtrA (23). *B. abortus*, while itself a nonmotile species, encodes some elements of the flagellar biosynthesis pathway (19). *S. meliloti* has hierarchical assembly of flagella, expression of which is essential for establishment of nitrogen-fixing nodules on roots of legumes (49); regulation by CtrA is unknown, although it is predicted based on potential CtrA binding sites (6).

The recently sequenced genomes of two deeply branching alphaproteobacteria, *Odyssella thessalonicensis* and *Midichloria mitochondrii*, pose intriguing questions regarding the origin of motility in the *Alphaproteobacteria* and the transition to intracellular lifestyles. *M. mitochondrii* diverged ancestrally to the *Rickettsiales*, and while it adopts an intracellular lifestyle, it retains a full complement of flagellar biosynthesis genes, some of which are possibly expressed inside host tissues (43). This organism, however, does not encode a definitive CtrA homolog; on the other hand, *O. thessalonicensis*, which by 16S phylogeny is placed between the *Rickettsiales* and the rest of the *Alphaproteobacteria*, does possess a CtrA homolog in addition to some flagellar biosynthesis genes (16).

In light of these new findings, we can posit that the ancestral alphaproteobacterium was motile and during its evolutionary journey acquired regulation of motility by the response regulator CtrA. In the *Rickettsiales* and protomitochondrial lineages, the necessity for motility was removed upon the transition to intracellular lifestyles, and the flagellar biosynthesis genes were lost.

Amino acid sequence across the C-terminal domains of CtrA in alphaproteobacteria is highly conserved (Fig. 2B), and identified CtrA binding sites are quite similar among species in which they have been determined. Therefore, it appears likely that the divergent cellular functions adopted by CtrA across the phyla are due not to divergent properties of CtrA itself but rather to the promoter sequences of the genes on which it exerts transcriptional control. Regulation of CtrA's activity, no doubt, will also vary between species due to differences in the upstream phosphorelay signals that it receives, but the output will be determined chiefly by the presence or absence of a CtrA binding motif in the promoter region of target genes (6). In AMB-1, these targets are primarily genes with motility, metabolic, or unknown functions and bear little overlap with regulons of species in which CtrA plays direct roles in DNA replication and cell division. In species where CtrA is essential for those processes, the regulation of CtrA's activity is more intricately controlled through checks and balances of protein levels, localization, and the phosphorylation state than is predicted for species in which CtrA plays a more accessory role in the organism's lifestyle (6). AMB-1 potentially occupies an intermediary evolutionary niche, since gene expression results and bioinformatic predictions suggest control of DNA methylation through CcrM, although CtrA is likely not the only regulator of this process, since CcrM expression remained even in the absence of CtrA.

The results of the study presented here are the most comprehensive experimental examination of a putative CtrA regulon in an organism in which the protein is not essential. As such, they have provided a glimpse into the evolution and divergent specialization of this important regulator and provide the basis for future detailed mechanistic studies into its function in AMB-1.

ACKNOWLEDGMENTS

We acknowledge members of the Komeili lab for careful reading of the manuscript and members of Kathleen Ryan's lab for helpful discussion.

Arash Komeili is supported by the NIH (NIGMS R01GM084122) and by a David and Lucille Packard Foundation Fellowship in Science and Engineering. Shannon Greene was supported by NIH Genetics Training Grant GM07127. Matteo Brilli was supported by ERC Advanced Grant SISYPHE and by ANR project MIRI, ANR-08-BLAN-0293-01.

REFERENCES

1. **Barnett MJ, Hung DY, Reisenauer A, Shapiro L, Long SR.** 2001. A homolog of the CtrA cell cycle regulator is present and essential in *Sinorhizobium meliloti*. J. Bacteriol. **183**:3204–3210.
2. **Bellefontaine AF, et al.** 2002. Plasticity of a transcriptional regulation network among alpha-proteobacteria is supported by the identification of CtrA targets in *Brucella abortus*. Mol. Microbiol. **43**:945–960.
3. **Biondi EG, et al.** 2006. Regulation of the bacterial cell cycle by an integrated genetic circuit. Nature **444**:899–904.
4. **Bird T, MacKrell A.** 2011. A CtrA homolog affects swarming motility and encystment in *Rhodospirillum centenum*. Arch. Microbiol. **193**:451–459.
5. **Bolstad BM, Irizarry RA, Astrand M, Speed TP.** 2003. A comparison of normalization methods for high density oligonucleotide array data based on variance and bias. Bioinformatics **19**:185–193.
6. **Brilli M, et al.** 2010. The diversity and evolution of cell cycle regulation in alpha-proteobacteria: a comparative genomic analysis. BMC Syst. Biol. **4**:52.
7. **Chen YE, et al.** 2011. Spatial gradient of protein phosphorylation underlies replicative asymmetry in a bacterium. Proc. Natl. Acad. Sci. U. S. A. **108**:1052–1057.
8. **Cheng Z, Miura K, Popov VL, Kumagai Y, Rikihisa Y.** 2011. Insights into the CtrA regulon in development of stress resistance in obligatory intracellular pathogen *Ehrlichia chaffeensis*. Mol. Microbiol. **82**:1217–1234.
9. **Curtis PD, Brun YV.** 2010. Getting in the loop: regulation of development in *Caulobacter crescentus*. Microbiol. Mol. Biol. Rev. **74**:13–41.
10. **Domian IJ, Quon KC, Shapiro L.** 1997. Cell type-specific phosphorylation and proteolysis of a transcriptional regulator controls the G1-to-S transition in a bacterial cell cycle. Cell **90**:415–424.
11. **Domian IJ, Reisenauer A, Shapiro L.** 1999. Feedback control of a master bacterial cell-cycle regulator. Proc. Natl. Acad. Sci. U. S. A. **96**:6648–6653.
12. **Edgar RC.** 2004. MUSCLE: multiple sequence alignment with high accuracy and high throughput. Nucleic Acids Res. **32**:1792–1797.
13. **Felsenstein J.** 1985. Confidence limits on phylogenies: an approach using the bootstrap. Evolution **39**:783–791.
14. **Frankel RB, Bazylinski DA, Schüler D.** 1998. Biomineralization of magnetic iron minerals in bacteria. Supramol. Sci. **5**:383–390.
15. **Fukuda Y, Okamura Y, Takeyama H, Matsunaga T.** 2006. Dynamic analysis of a genomic island in *Magnetospirillum* sp. strain AMB-1 reveals how magnetosome synthesis developed. FEBS Lett. **580**:801–812.
16. **Georgiades K, Madoui M-A, Le P, Robert C, Raoult D.** 2011. Phylogenomic analysis of *Odyssella thessalonicensis* fortifies the common origin of *Rickettsiales*, *Pelagibacter ubique* and *Reclimonas americana* Mitochondrion. PLoS One **6**:e24857.

17. **Gitai Z, Dye NA, Reisenauer A, Wachi M, Shapiro L.** 2005. MreB actin-mediated segregation of a specific region of a bacterial chromosome. Cell **120**:329.
18. **Hallez R, Bellefontaine A-F, Letesson J-J, De Bolle X.** 2004. Morphological and functional asymmetry in α-Proteobacteria. Trends Microbiol. **12**:361–365.
19. **Halling SM.** 1998. On the presence and organization of open reading frames of the nonmotile pathogen *Brucella abortus* similar to class II, III, and IV flagellar genes and to LcrD virulence superfamily. Microb. Comp. Genomics **3**:21–29.
20. **Irizarry RA, et al.** 2003. Summaries of Affymetrix GeneChip probe level data. Nucleic Acids Res. **31**:e15.
21. **Irizarry RA, et al.** 2003. Exploration, normalization, and summaries of high density oligonucleotide array probe level data. Biostatistics **4**:249–264.
22. **Jones DT, Taylor WR, Thornton JM.** 1992. The rapid generation of mutation data matrices from protein sequences. Comput. Appl. Biosci. (Camb.) **8**:275–282.
23. **Kahng LS, Shapiro L.** 2001. The CcrM DNA methyltransferase of *Agrobacterium tumefaciens* is essential, and its activity is cell cycle regulated. J. Bacteriol. **183**:3065–3075.
24. **Kelly AJ, Sackett MJ, Din N, Quardokus E, Brun YV.** 1998. Cell cycle-dependent transcriptional and proteolytic regulation of FtsZ in Caulobacter. Genes Dev. **12**:880–893.
25. **Komeili A, Li Z, Newman DK, Jensen GJ.** 2006. Magnetosomes are cell membrane invaginations organized by the actin-like protein MamK. Science **311**:242.
26. **Komeili A, Vali H, Beveridge TJ, Newman DK.** 2004. Magnetosome vesicles are present before magnetite formation, and MamA is required for their activation. Proc. Natl. Acad. Sci. U. S. A. **101**:3839–3844.
27. **Lang AS, Beatty JT.** 2002. A bacterial signal transduction system controls genetic exchange and motility. J. Bacteriol. **184**:913–918.
28. **Lang AS, Beatty JT.** 2000. Genetic analysis of a bacterial genetic exchange element: the gene transfer agent of Rhodobacter capsulatus. Proc. Natl. Acad. Sci. U. S. A. **97**:859–864.
29. **Laub MT, Chen SL, Shapiro L, McAdams HH.** 2002. Genes directly controlled by CtrA, a master regulator of the Caulobacter cell cycle. Proc. Natl. Acad. Sci. U. S. A. **99**:4632–4637.
30. **Laub MT, McAdams HH, Feldblyum T, Fraser CM, Shapiro L.** 2000. Global analysis of the genetic network controlling a bacterial cell cycle. Science **290**:2144–2148.
31. **Liu XS, Brutlag DL, Liu JS.** 2002. An algorithm for finding protein-DNA binding sites with applications to chromatin-immunoprecipitation microarray experiments. Nat. Biotechnol. **20**:835–839.
32. **Matsunaga T, Sakaguchi T, Tadokoro F.** 1991. Magnetite formation by a magnetic bacterium capable of growing aerobically. Appl. Environ. Microbiol. **35**:651–655.
33. **Mercer RG, et al.** 2010. Loss of the response regulator CtrA causes pleiotropic effects on gene expression but does not affect growth phase regulation in *Rhodobacter capsulatus*. J. Bacteriol. **192**:2701–2710.
34. **Miller TR, Belas R.** 2006. Motility is involved in *Silicibacter* sp. TM1040 interaction with dinoflagellates. Environ. Microbiol. **8**:1648–1659.
35. **Murat D, Byrne M, Komeili A.** 2010. Cell biology of prokaryotic organelles. Cold Spring Harb. Perspect. Biol. **2**:a000422.
36. **Murat D, Quinlan A, Vali H, Komeili A.** 2010. Comprehensive genetic dissection of the magnetosome gene island reveals the step-wise assembly of a prokaryotic organelle. Proc. Natl. Acad. Sci. U. S. A. **107**:5593–5598.
37. **Philippe N, Wu L-F.** 2010. An MCP-like protein interacts with the MamK cytoskeleton and is involved in magnetotaxis in *Magnetospirillum magneticum* AMB-1. J. Mol. Biol. **400**:309–322.
38. **Quon KC, Marczynski GT, Shapiro L.** 1996. Cell cycle control by an essential bacterial two-component signal transduction protein. Cell **84**:83–93.
39. **Quon KC, Yang B, Domian IJ, Shapiro L, Marczynski GT.** 1998. Negative control of bacterial DNA replication by a cell cycle regulatory protein that binds at the chromosome origin. Proc. Natl. Acad. Sci. U. S. A. **95**:120–125.
40. **Robertson GT, et al.** 2000. The *Brucella abortus* CcrM DNA methyltransferase is essential for viability, and its overexpression attenuates intracellular replication in murine macrophages. J. Bacteriol. **182**:3482–3489.
41. **Ryan KR, Huntwork S, Shapiro L.** 2004. Recruitment of a cytoplasmic response regulator to the cell pole is linked to its cell cycle-regulated proteolysis. Proc. Natl. Acad. Sci. U. S. A. **101**:7415–7420.
42. **Santos SR, Ochman H.** 2004. Identification and phylogenetic sorting of bacterial lineages with universally conserved genes and proteins. Environ. Microbiol. **6**:754–759.
43. **Sassera D, et al.** 2011. Phylogenomic evidence for the presence of a flagellum and cbb3 oxidase in the free-living mitochondrial ancestor. Mol. Biol. Evol. **28**:3285–3296.
44. **Sato R, et al.** 1995. Synchronous culture of *Magnetospirillum* sp. AMB-1 by repeated cold treatment. FEMS Microbiol. Lett. **128**:15–19.
45. **Scheffel A, Gardes A, Grunberg K, Wanner G, Schüler D.** 2008. The major magnetosome proteins MamGFDC are not essential for magnetite biomineralization in Magnetospirillum gryphiswaldense but regulate the size of magnetosome crystals. J. Bacteriol. **190**:377–386.
46. **Shelswell KJ, Taylor TA, Beatty JT.** 2005. Photoresponsive flagellum-independent motility of the purple phototrophic bacterium *Rhodobacter capsulatus*. J. Bacteriol. **187**:5040–5043.
47. **Siam R, Marczynski GT.** 2003. Glutamate at the phosphorylation site of response regulator CtrA provides essential activities without increasing DNA binding. Nucleic Acids Res. **31**:1775–1779.
48. **Smith MJ, et al.** 2006. Quantifying the magnetic advantage in magnetotaxis. Biophys. J. **91**:1098–1107.
49. **Sourjik V, Muschler P, Scharf B, Schmitt RD.** 2000. VisN and VisR are global regulators of chemotaxis, flagellar, and motility genes in *Sinorhizobium* (*Rhizobium*) *meliloti*. J. Bacteriol. **182**:782–788.
50. **Stephens CM, Zweiger G, Shapiro L.** 1995. Coordinate cell cycle control of a *Caulobacter* DNA methyltransferase and the flagellar genetic hierarchy. J. Bacteriol. **177**:1662–1669.
51. **Tamura K, et al.** 2011. MEGA5: molecular evolutionary genetics analysis using maximum likelihood, evolutionary distance, and maximum parsimony methods. Mol. Biol. Evol. **28**:2731–2739.
52. **Ullrich S, Kube M, Schübbe S, Reinhardt R, Schüler D.** 2005. A hypervariable 130-kilobase genomic region of *Magnetospirillum gryphiswaldense* comprises a magnetosome island which undergoes frequent rearrangements during stationary growth. J. Bacteriol. **187**:7176–7184.
53. **Whelan S, Goldman N.** 2001. A general empirical model of protein evolution derived from multiple protein families using a maximum-likelihood approach. Mol. Biol. Evol. **18**:691–699.
54. **White CL, Kitich A, Gober JW.** 2010. Positioning cell wall synthetic complexes by the bacterial morphogenetic proteins MreB and MreD. Mol. Microbiol. **76**:616–633.
55. **Wolfe RS, Thauer RK, Pfennig N.** 1987. A "capillary racetrack" method for isolation of magnetotactic bacteria. FEMS Microbiol. Lett. **45**:31–35.
56. **Yang C-D, Takeyama H, Tanaka T, Hasegawa A, Matsunaga T.** 2001. Synthesis of bacterial magnetic particles during cell cycle of *Magnetospirillum magneticum* AMB-1. Appl. Biochem. Biotechnol. **91**:155–160.